Colloid & Polymer Sci: **258**, 1335–1342 (1980)

ISSN 0303-402X / ASTM-Coden: CPMSB (formerly KZZPAF)

Polymer Engineering The University of Tennessee Knoxville, Tennessee, USA

Phase behavior and structure of liquid crystalline solutions of cellulose derivatives

J. Bheda, J. F. Fellers, and *J. L. White*

With 5 figures and 4 tables

(Received Spetember 19, 1980)

Introduction

Liquid crystalline polymer materials have attracted considerable attention during the past decade. Such characteristics have now been found in a range of polymers including polypeptides (1–3), *p*-linked aromatic polyamides (3–10), aromatic polyesters (10–12) and other polycondensates.

The great interest in polymer liquid crystals has been associated with their ability to form high modulus and tensile strength fibers (4–8, 10, 12). The DuPont fiber Kevlar® is a *p*-linked aromatic polyamide formed by wet spinning of a liquid crystalline solution of the polymer.

Werbowyj and *Gray* (13, 14) have found that hydroxypropyl cellulose (HPC) solutions in water are cholesteric liquid crystals at high concentration. Liquid crystal formation was also noted in ethanol and methanol (14). *Panar* and *Willcox* (15) have shown that a large number of different cellulose derivatives form liquid crystalline solutions and investigated the formation of fibers from such solutions. Effects of solvent on the critical concentration of cellulose acetate solutions has very recently been described by *Aharoni* (16). *Chanzy* and his coworkers (17) have shown that cellulose itself forms liquid crystals in an N-methyl morpholine N-oxide solution. In earlier studies from our laboratories on liquid crystalline solutions we have examined aqueous solutions of HPC under quiescent conditions using polarized light microscopy, small angle light scattering (SALS) and optical density measurements (3) and in shear and elongational flow using flow birefringence (18).

We now report on the structural and thermodynamic characteristics of liquid crystalline solutions of four cellulose derivatives in a range of solvents. Basic observations were made on these systems using hot stage polarized light microscopy, small angle light scattering, dilute solution and concentrated solution viscosities. The polymers studied include hydroxypropyl cellulose (HPC), cellulose acetate butyrate (CAB), ethyl cellulose (EC) and cellulose triacetate (CT). This study continues our investigations of the polymer liquid crystalline state (3, 5, 10, 18–20).

Experimental

Materials

Four different cellulose derivatives were used in this study. These were a hydroxypropyl cellulose (HPC) of a degree of substitution three obtained from Hercules (Klucel L), a cellulose acetate butyrate (CAB) obtained from Tennessee Eastman, cellulose triacetate (CT) obtained from Celanese and ethyl cellulose (EC) obtained from Dow Chemical (Ethocel). These were studied in solutions formed from a range of solvents including dimethyl acetamide (DMA) (Aldrich) dichloracetic acid (DCA) (Aldrich), ethyl alcohol (denatured, Aldrich) methyl ethyl ketone (MEK) (Aldrich), acetic acid (Fisher) and water (distilled). The polymer-solvent pairs studied are summarized in table 1.

Procedures

Polarized light microscopy studies were performed with a Leitz Ortholux microscope. The solutions were placed in Fisher Scientific Littman glass slides containing a 600 μm deep cavity and covered with a thin glass slide. These were hermetically sealed with glue. Some samples of thickness 70 μm were also prepared using flat microscope slides and spacers. The characteristics were studied both at room

Table 1. Cellulose derivative-solvent pairs investigated

Polymer	Solvents
Hydroxypropyl Cellulose (HPC)	H_2O, CH_3COOH, C_2H_5OH Dimethyl acetamide (DMA) Dichloracetic Acid (DCA)
Cellulose Acetate Butyrate (CAB)	CH_3COOH, Methylethylketone (MEK) Dimethyl acetamide (DMA)
Ethyl Cellulose (EC)	CH_3COOH, Dichloracetic Acid (DCA)
Cellulose Triacetate (CT)	Dichloracetic Acid

temperature and at elevated temperatures using a hot stage. Transmitted light intensities were measured with a photometer.

SALS studies were carried out using a helium neon gas laser on an optical bench with a polarizer, sample holder, analyzer and photographic film (Polaroid No. 55). The assembly was within a lightproof box where it was possible to vary the sample to film distance from 5 to 70 cm.

Dilute solution viscosities for the various polymer-solvent systems were measured with an Ubbeholde viscometer at 25 ± 0.1 °C.

Steady shear viscosities were obtained at room temperature using a Rheometrics Mechanical Spectrometer.

Phase transitions

Results

At low concentrations all solutions are found by the polarized light microscope to be optically isotropic and to pass no polarized light. At a critical concentration C_A (gms/ml) or volume fraction ϕ_A light begins to pass through and a morphology is observed. Thus C_A corresponds to the onset of the biphasic region (1–9). As concentration increases the amount of light passing through the solution increases until an asymptote is reached and this is designated as C_B (ϕ_B). Table 2 lists the values obtained for C_A, C_B, ϕ_A and ϕ_B. The critical concentrations for the polymer are dependent upon solvent. For HPC the value of C_A (ϕ_A) varies from 0.21 gms/ml (0.19) in dichloracetic acid, to 0.30 gms/ml (0.27) in acetic acid, to 0.38 gms/ml (0.35) in dimethylacetamide to 0.42 gms/ml (0.39) in H_2O and ethyl alcohol. For CAB, C_A varies from 0.38 gms/ml in dimethyl acetamide to 0.46 gms/ml in acetic acid to 0.50 gms/ml in methyl ethyl ketone. Similarly EC has a value of 0.30 gms/ml for dichloracetic acid and 0.40 gms/ml for acetic acid.

The C_A values are temperature dependent. Table 3 summarizes data for different systems. For HPC-DMA, C_A varies from 0.38 to 0.57 as temperature increases from room temperature to 120 °C. A similar but less pronounced trend is found in HPC/CH_3COOH.

Table 3. Critical concentrations for the onset of anisotropic phase in hydroxypropylcellulose solutions

Polymer	Solvent	Temperature	C_A
HPC	CH_3COOH	25 °C	0.30
		40 °	0.315
		38 °	0.32
		110 °	0.35
HPC	DMA	25 °	0.38
		40 °	0.40
		60 °	0.45
		75 °	0.50
		120 °	0.57

Table 2. Critical concentrations for the onset of the anisotropic phase in different cellulose derivative-solvent systems

Polarized Light Measurements							Solution Viscosity Maximum Minimum	
Polymer	Solvent	C_A (gms/ml)	ϕ_A	C_B (gms/ml)	ϕ_B	(dl/g) $[\eta]$ (25 °C)	C_A (gms/ml)	C_B (gms/ml)
HPC	DCA	0.21	0.19	0.25	0.23	1.83	–	–
	CH_3COOH	0.30	0.27	0.40	0.37	1.70	0.30	0.375
	DMA	0.38	0.35	0.50	0.465	1.40	0.38	0.45
	H_2O	0.42	0.39	0.54	0.51	1.23	–	–
	C_2H_5OH	0.43	0.395	0.54	0.51	1.25	–	–
CAB	DMA	0.38	0.34	0.45	0.40	2.12	0.30	0.45
	CH_3COOH	0.46	0.43	–	–	2.01	–	–
	MEK	0.50	0.46	–	–	1.74	–	–
EC	DCA	0.30	0.28	0.40	0.38	3.05	–	–
	CH_3COOH	0.40	0.39	0.475	0.46	2.24	0.40	0.45
CTA	DCA	0.38	0.35	–	–	3.57	–	–

The steady shear viscosity as a function of concentration shows a maximum in the neighborhood of the phase transformation. The viscosity then moves through a minimum before increasing again. Data for the positions of the maxima and minima are listed in table 2. For HPC/DMA the maximum is at a concentration of 0.39 gms/ml, for HPC/CH_3COOH it is at 0.30, for CAB/DMA it is 0.38 and for EC/CH_3COOH at 0.40. This closely corresponds to the polarized light microscopy data for C_A for these systems in table 2. Viscosity minima in the same three systems occurred at concentrations of 0.45, 0.375 and 0.45 gms/ml which are lower than the C_B values in table 2.

Discussion

Solvent dependences of ϕ_A

The critical concentrations for the formation of the liquid crystalline phase are found to be rather large compared to those found in PγBLG and aromatic polyamide solutions (1-10) where values are generally of order $\phi<0.1$. This agrees with the observations of *Onogi* et al. (3) and *Panar* and *Willcox* (15) on similar systems. The variation of critical concentration of cellulose derivatives with solvent has also been noted by *Aharoni* (16).

The results of table 2 are of considerable interest. According to the generally accepted lattice formulation of *Flory* (21), the critical concentrations of polymer solution should be largely independent of solvent and only dependent upon polymer volume fraction. *Wirick* and *Waldman* (24) have developed an intrinsic viscosity molecular weight relationship for an HPC similar to that studied here using ethanol. An $[\eta]$ of 1.25 is equivalent to a weight average molecular weight of 85,000 and an aspect ratio, χ, of 135. According to Flory's expression

$$\phi_A = \frac{8}{x}\left(1 - \frac{2}{x}\right) \qquad [1]$$

ϕ should be about 0.06. The values of table 2 for HPC range from 0.19 to 0.39. It is not conceivable that molecular weight distribution effects could cause such a discrepancy. It may be argued that it is doubtful whether the specific formulations published by *Flory* should be applied to solutions of cellulose derivatives in the types of solvents listed in table 1. This is because of obviously major polarity effects in these systems.

From table 2, we see that the critical concentration C_A or ϕ_A for the HPC, CAB and EC solutions depends upon the intrinsic viscosity for that polymer-solvent combination. Clearly the larger $[\eta]$, the smaller the value of C_A (ϕ_A).

The large values of ϕ_A and the dependence upon $[\eta]$ can be acommodated to the general perspective of *Flory* (21) by hypothesizing that polymer chain flexibility is strongly affected by solvent interaction. More acid solvents tend to increase end-to-end distance, chain rigidity and effective aspect ratio. Solvent effects order according to

$$\text{DCA} > CH_3COOH > \text{DMA} > H_2O > C_2H_5OH$$

for HPC, CAB and EC. Mechanistically this could occur because of protonation of the cellulose derivative molecule with chain expansion occurring because of electrostatic repulsion.

Another explanation for the variation of ϕ_A lies in the possible existence of association in non-acid solvents which decreases the effective aspect ratio of the macromolecules.

The viscosity-concentration curves which exhibit maxima and minima resemble those obtained by earlier researchers on polymer liquid crystalline solutions (5–10, 15, 19–20). Interestingly they also resemble the viscosity-conversion plots for polymerization of styrene solutions of elastomers (22, 23). This occurs in the bulk polymerization of high impact polystyrene. The maxima/minima correspond to a phase inversion in which low viscosity polystyrene solutions become the continuous phase.

Temperature dependence of transition

From table 3, it may be seen that there is a strong temperature dependence of the critical concentrations in the HPC/DMA solution and a rather milder dependence in the HPC/CH_3COOH system. From classical solution thermodynamics (25), it may be shown that the temperature dependence of the critical concentration is an increasing function of the heat of transformation. This follows from equating the

chemical potentials (or fugacities) of the solvent in the isotropic and liquid crystalline phases. An expression of the form

$$\frac{\partial \ln(a)}{\partial T} = -\frac{\Delta H}{RT^2}$$

is obtained where ΔH is the heat of the transformation and a, the activity at the transformation. If we use another equilibrium quantity, $\varnothing_A$, instead of activity, a value of ΔH of -60 calories/gram mole in HPC/CH_3COOH and -850 calories/gram mole in HPC/DMA is calculated.

Two phase region

It is clear from table 2 that the two phase region increases in width as C_A ($\varnothing_A$) increases. For HPC in DCA, the range ($\varnothing_B - \varnothing_A$) is 0.04 but it monotonically increases to a value of 0.12 in C_2H_5OH and H_2O. A small ($\phi_B - \phi_A$) corresponds to large acidity and large $[\eta]$.

Structure of liquid crystalline solutions

Results

Appearance

Generally the liquid crystalline solutions are cloudy. Some solutions show iridescent colors over a range of concentrations. This is especially striking in HPC-H_2O solutions which are highly colored at concentrations of 0.60–0.65. (This has been noted by earlier investigators (3, 13, 14, 18)). Similar colors are observed in HPC-CH_3COOH but only at concentrations of 0.80. Colors range from red to violet. Faint iridescent colors are also observed in the HPC-DMA solutions at concentrations of 0.60 and greater. Faint iridescent colors are seen in the EC-CH_3COOH solutions in the concentration range of 0.47–0.50

Polarized light microscopy

It is of greatest interest to compare the characteristics of different liquid crystalline solutions of the same polymer. First we compare the HPC systems. All of the HPC solutions exhibit what appear to be spherulitic domain structures in concentrated solutions (fig. 1). The spherulites are negative, i.e. the tangential refractive index n_θ is greater than the radial refractive index n_r. The morphologies of the HPC-DCA and HPC-CH_3COOH are better defined than those of the other solutions and contain a well resolved 'finger print' pattern of parallel lines at lower concentrations (fig. 2). These are not seen in the other HPC systems. Spherulite sizes are summarized in table 4.

The EC solutions show a very detailed and distinct morphology. Well defined spherulites are observed in the two-phase region. These spherulites are negative as in the case of the HPC solutions and have diameters ranging from 2 um to 35 μm. Annealing of the two phase region in both EC-CH_3COOH and EC-DCA solutions result in ringed domains containing fingerprint patterns similar to those observed in solutions of HPC in the same solvents (see Fig. 3). The EC-CH_3COOH solutions become completely anisotropic at a concentration of 0.42 gms/ml where they have a speckled appearance. In the EC-DCA solutions, the systems

Table 4. Cellulose derivative liquid crystals spherulite size from polarized light microscopy and SALS

Polymer	Solvents	Conc'n (gms/ml)	Domain (Spherulite) Size, μm Polarized light microscopy	SALS
HPC	DMA	0.45	12	
		0.50	21	
		0.70		35
HPC	CH_3COOH	0.315	2.5	
EC	CH_3COOH	0.40		1.0
		0.45		2.0
		0.50		3.0
EC	DCA	0.30	10	10
CT	DCA	0.35	9	10

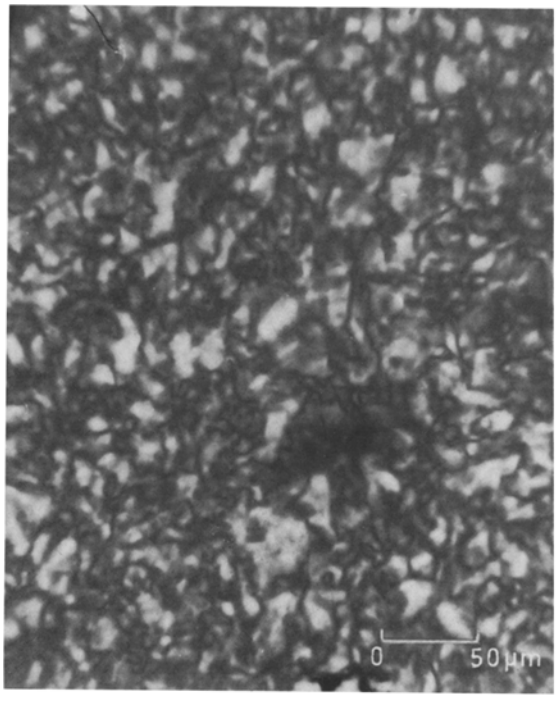

1a

Fig. 2. Polarized light optical photomicrograph of HPC in acetic acid at 0.325 gm/ml

1b

Fig. 1. Polarized light optical photomicrographs of HPC solutions. (a) HPC in dimethyl acetamide at 0.70 gm/cm^3 (b) HPC in acetic acid at 0.70 gm/cm^3

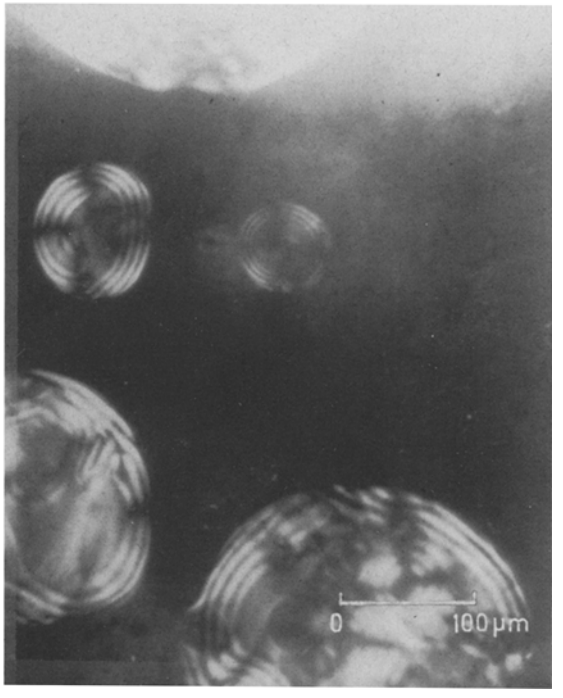

Fig. 3. 35 weight percent solution of ethyl cellulose in dichoracetic acid at 37 °C showing ringed domains containing fingerprint patterns

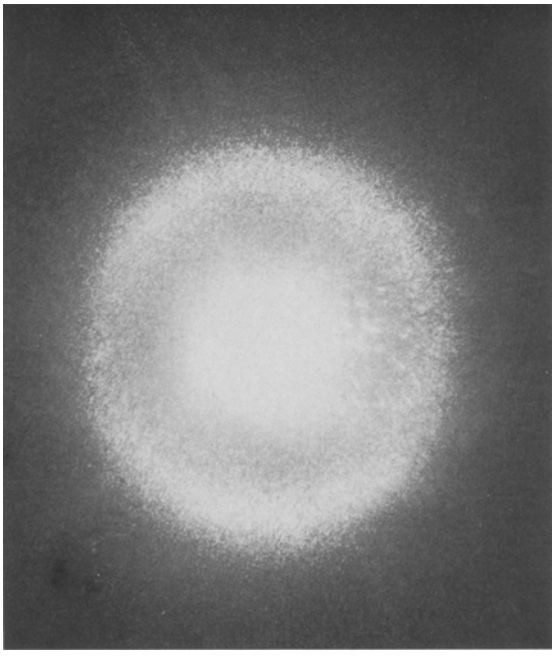

Fig. 4. SALS pattern for HPC in acetic acid at 0.325 gms/ml. The camera to sample distance was 11 cm

become completely anisotropic at a concentration of 0.40. From concentrations of 0.40 to 0.45 a fingerprint structure of parallel lines is observed. At higher concentrations a 'speckled' structure is observed.

In CT-DCA solutions, well defined spherulites are observed in the twophase systems. At concentrations of 0.40 these have diameters of 10 μm. There are positive spherulites, i.e. the radial refractive index is greater than the tangential refractive index, $n_r > n_\theta$. The spherulites have fingerprint structures. At concentrations of 0.50 the appearance of the now completely anisotropic phase is speckled in character.

The CAB solutions have the least well defined structures. Spherulites are not observed. Indeed one can only characterize an increasing brightness with concentration.

SALS

HPC solutions in CH_3COOH, DMA and H_2O exhibit 'four petal' H_v SALS patterns over certain concentration ranges. These are probably best defined in the CH_3COOH solutions. The CH_3COOH SALS patterns have the most interesting characteristics. At higher concentration a ring appears beyond the four petal structure (fig. 4). (The HPC–DMA and HPC-C_2H_5OH solutions were not studied in this experiment).

Well defined four petal patterns are also seen in EC-CH_3COOH solutions (fig. 5) which decrease in size with increasing concentration as well as in EC-DCA and CT-DCA solutions. No distinct H_v SALS patterns were obtained in the CAB solutions.

Interpretation

It is possible to develop considerable information about the arrangement of the macromolecules from the observations described above. Oriented filaments of HPC exhibit positive birefringence (compare *Onogi* et al. (18)) as do filaments of EC. The refractive index along the axis n_z is greater than the radial refractive index n_r. CT filaments on the other hand have a negative birefringence, i.e. $n_r > n_z$. As HPC and EC solutions have negative spherulites and CT solutions have positive spherulites, if we presume birefringence is dominated by molecular polarizability rather than form birefringence, (compare *Onogi* et al. (18)) the above results lead to the conclusion the macromolecules of HPC, ET and CT are arranged tangentially within the spherulites.

The existence of spherulitic structures is also supported by the SALS H_v four petal patterns

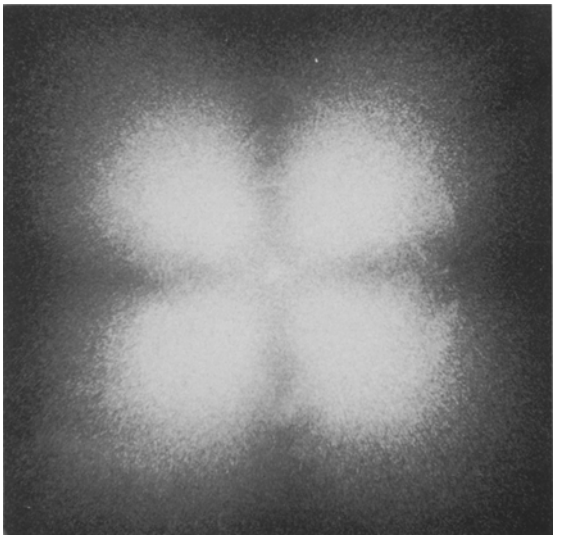

Fig. 5. SALS pattern for a 0.40 gms/ml ethyl cellulose solution in acetic acid. The sample camera distance was 5.5 cm

with intensity maxima in the petals (26–28). This we determined by using the variation of optical density of photographic negatives. Spherulite diameters have been computed and are summarized in table 4.

The colors exhibited by the HPC and EC solutions suggest the cholesteric character of these solution. This has been confirmed for HPC-H_2O solutions by earlier investigators (3, 13). The parallel layer fingerprint structures observed in our solutions are strongly reminiscent of observations by *Robinson* (1) and others on PγBLG solutions. Lamellar structures were interpreted in terms of cholesteric pitch. SALS H_v patterns show rings corresponding to similar Bragg distances. In some cases SALS H_v patterns have an inner (smaller angle) four petal pattern and an outer (larger angle) ring. From Bragg's Law this would appear to correspond to spherulites containing cholesteric layered structures. Similar SALS observations on PγBLG solutions have been made by *Onogi* et al. (3). The computed pitches are similar to those obtained from lamellar spacings.

Concluding remarks

The significance of polymer structural regularity, polymer-solvent interaction, and polymer-polymer interaction in the liquid crystal character of the cellulose derivative-solutions become apparent with the following phenomenological summary. The intrinsic viscosity varies inversely with $\varnothing_A$. for a particular polymer in a series of solvents. The value of $\varnothing_A$ correlates with solvent acidity. Also not only $\varnothing_A$ correlates with solvent acidity, but $\varnothing_B - \varnothing_A$ changes with solvent acidity. A negative ΔH for the onset of liquid crystal formation was determined and it depended on solvent chemical type. Finally, the degree of structural fineness or resolution of the liquid crystal, as observed in the optical microscope, increases as the polymer solid state crystallinity orders from CAB (amorphous) to CT (crystalline) to EC (more crystalline). This structural fineness also increases with solvent acidity.

Summary

Structural and thermodynamic characteristics of liquid-crystalline solutions of four cellulose derivatives in a range of solvents were studied. Basic observations were made on these systems using polarized light microscopy, small angle light scattering, dilute solution and concentrated solution viscosities. The polymers studied include hydroxypropyl cellulose (HPC), cellulose acetate butyrate (CAB), ethyl cellulose (EC), and cellulose triacetate (CT). The formation of the liquid crystalline phase was shown to strongly depend on polymer concentration, solvent type and temperature. The critical volume fraction of polymer required to form the liquid crystal phase varied significantly as the solvent changed. The critical volume fraction decreased with increasing solvent acidity and polymer intrinsic viscosity in a given solvent. The breadth of the two phase region seems to decrease with increasing acidity. The liquid crystalline phase was in most cases determined to be cholesteric. In all cases positively birefringent cellulose derivatives form negative spherulitic domains. In one case, the negativity birefringent system (cellulose triacetate) formed positively birefringent spherulitic liquid crystalline domains. This is interpreted to mean the structure organizes itself by a tangential alignment of polymer chains within the domain. SALS measurements appear to detect domains and in some cases cholesteristic pitch.

References

1) *Robinson, C.*, Trans. Faraday Soc. **52**, 571 (1956), Tetrahedron **13**, 219 (1961).

2) *Samulski E. T., A. V. Tobolsky*, in: Liquid Crystals and Plastic Crystals edited by G. Gray and P. Winsor, Wiley, NY (1974).

3) *Onogi, Y., J. L. White, J. F. Fellers*, J. Polym. Sci. Polym. Phys. **18**, 663 (1980).

4) *Kwolek, S. L.*, U. S. Patent, 3, 671, 542 (1972).

5) *Hancock, T. A., J. E. Spruiell, J. L. White*, J. Appl. Polym. Sci. **21**, 1227 (1977).

6) *Morgan, P. W.*, Macromolecules **10**, 1381 (1977).

7) *Kwolek, S. L., P. W. Morgan, J. R. Shaefgen, L. W. Gulrich*, Macromolecules **10**, 1390 (1977).

8) *Bair, T. I., P. W. Morgan, F. L. Killian*, Macromolecules **10**, 1396 (1977).

9) *Panar, M., L. F. Beste*, Macromolecules **10**, 1401 (1977).

10) *White, J. L., J. F. Fellers*, Appl. Polym. Symp. **33**, 137 (1978).

11) *Jackson, W. J., H. F. Kuhfuss*, J. Polym. Sci. Polym. Chem. **14**, 2043 (1976).

12) *Pletcher, T. C.*, U. S. Patent, 3, 991, 013 (1976), and *J. J. Kleinschuster*, U.S. Patent, 3, 991, 014 (1976).

13) *Werbowyj, R. S., D. G. Gray*, Mol. Cryst, Liq. Cryst. **34**, (Letters) 97 (1976).

14) *Werbowyj, R. S., D. G. Gray*, Macromolecules **13**, 69 (1980).

15) *Panar, M., O. B. Willcox*, Offenlegungsschrift, 2705381, German Federal Republic (1977).

16) *Aharoni, S. M.*, Mol. Cryst. Liq. Cryst. **56**, (Letters) 237 (1980).

17) *Chanzy, H., M. Dube, R. H. Marchessault*, J. Polym. Sci., Polym. Letters **17**, 219 (1979).

18) *Onogi, Y., J. L. White, J. F. Fellers*, J. Non-Newt. Fluid Mech. **7**, 121 (1980).

19) *Aoki, H., J. L. White, J. F. Fellers*, J. Appl. Polym. Sci. **23**, 2293 (1979).

20) *Aoki, H., Y. Onogi, J. L. White, J. F. Fellers,* Polym. Eng. Sci. **20**, 221 (1980).
21) *Flory, P. J.,* Proc. Roy. Soc. **A234**, 73 (1956).
22) *Bender, B. W.,* J. Appl. Polym. Sci. **9**, 2887 (1965).
23) *Molau, G. E., W. M. Witbrodt, V. E. Meyer,* J. Appl. Polym. Sci. **13**, 2735 (1969).
24) *Wirick, M. G., M. H. Waldman,* J. Appl. Polym. Sci. **14**, 579 (1970).
25) *Denbigh, K.,* The Principles of Chemical Equilibrium, 3rd Edition, Cambridge University Press (1971).
26) *Stein, R. S., M. B. Rhodes,* J. Appl. Phys. **31**, 1873 (1960).
27) *Samuels, R. J.,* J. Polym. Sci. A-2, **9**, 2165 (1971).
28) *Hashimoto, T., A. Todo, H. Kawai,* J. Polym. Sci. Polym. Phys. **11**, 149, (1973).

Author's addresses:

J. F. Fellers and J. L. White
Polymer Engineering
The University of Tennessee
Knoxville, Tennessee 37916

J. Bheda
TFE Corporation
Kalamazoo, Michigan
49006